Radiochim. Acta **89**, 625–631 (2001)


# EXAFS investigation of uranium(VI) complexes formed at *Bacillus cereus* and *Bacillus sphaericus* surfaces

By C. Hennig[1], P. J. Panak[1,†], T. Reich[1,*], A. Roßberg[1], J. Raff[1], S. Selenska-Pobell[1], W. Matz[2], J. J. Bucher[3], G. Bernhard[1] and H. Nitsche[1,†]

[1] Institute of Radiochemistry, Forschungszentrum Rossendorf, PF 510119, D-01314 Dresden, Germany
[2] Institute of Ion Beam Physics and Materials Research, Forschungszentrum Rossendorf, PF 510119, D-01314 Dresden, Germany
[3] Lawrence Berkeley National Laboratory, MS 70A-1150, Berkeley, CA 94720, USA

(Received May 25, 2000; accepted in final form April 23, 2001)

*EXAFS / Uranium complexation / Bacillus cereus / Bacillus sphaericus*

**Summary.** Uranium(VI) complex formation at vegetative cells and spores of *Bacillus cereus* and *Bacillus sphaericus* was studied using uranium $L_{II}$-edge and $L_{III}$-edge extended X-ray absorption fine structure (EXAFS) spectroscopy. A comparison of the measured equatorial U−O distances and other EXAFS structural parameters of uranyl species formed at the *Bacillus* strains with those of the uranyl structure family indicates that the uranium is predominantly bound as uranyl complexes with phosphoryl residues.

## Introduction

Bacteria in soil, sediment, and water have a significant influence on the transport of radionuclides and other heavy metals in nature [1]. Certain bacterial strains can selectively accumulate various metal ions from aqueous systems [2], and are, therefore, important for the regulation of environmental pollution and remediation. Because of the high resistance of their spores to extreme conditions, bacilli are found in a large variety of natural habitats. Recently, it was demonstrated that two *Bacillus* strains, *B. cereus* JG-A30 and *B. sphaericus* JG-A12, recovered from a uranium mining waste site in Germany, are able to accumulate selectively a large variety of heavy metals from the drain waters of the waste site [3]. In particular, it was shown that these strains accumulate large amounts of uranium. The uranyl sorption mechanism of the vegetative cells and of the spores of these bacteria is of great interest for the development of bacteria-based techniques for the removal of toxic metals from mill-tailings and waste water of uranium mines.

Our former study [4] showed that the uranium can be released almost quantitatively from vegetative cells and spores of bacilli by extraction with a strong complexing agent. This indicated that the uranium species were formed extracellular. Furthermore, that investigation showed by time-resolved laser-induced fluorescence spectroscopy (TRLFS) that uranium built inner-sphere complexes with phosphate groups of the biomass. This lead to the conclusion that phosphate residues of cell wall components of the Gram-positive bacteria *B. cereus* and *B. sphaericus* are responsible for the uranium binding.

The aim of this paper is to study the structure of uranium species formed at vegetative cells and spores of the above mentioned *Bacillus* strains using extended X-ray absorption fine structure (EXAFS) spectroscopy. Analytical procedures allow separating radial distribution functions, which contain information on bond lengths and coordination numbers, from the EXAFS. This radial distribution function is an average of all signals from different uranium coordination centers in the sample. However, frequently the EXAFS is dominated by the major coordination type in the sample. A comparison of the determined structural parameters with those of the uranium structure family allows analyzing the type of uranium species in the bacteria samples.

## Experimental

### Sample preparation

The uranium biosorption was investigated on indigenous *Bacillus* isolates, recovered from a uranium waste pile, the "Haberlandhalde" near the town of Johanngeorgenstadt in Saxony, Germany. Vegetative cells and spores of the isolates *B. cereus* JG-A30 and *B. sphaericus* JG-A12 were studied. For comparison, vegetative cells and spores of two reference strains *B. cereus* 4415 and *B. sphaericus* 9602 were analyzed as well. The *Bacillus* strains used are listed in Table 1. The *Bacillus* strains were grown with intensive aeration in 300 ml nutrient medium (8 g/l nutrient broth, Difco Laboratories, Augsburg, Germany) at 30 °C [4]. The bacterial biomass was separated from the growth medium using low speed centrifugation (6000 × g). For preparation of the EXAFS samples, the biomass was treated for two days with 50 ml of 0.9% NaCl-solution containing $10^{-4}$ mol/l U(VI) at pH 5. The biomass was separated from the growth medium by centrifugation. To remove ingredients of the

*Author for correspondence (E-mail: REICH@ESRF.FR).
† Current address: Lawrence Berkeley National Laboratory, MS 70A-1150, Berkeley, CA 94720, USA

**Table 1.** *Bacillus* strains used.

| Strain | Source |
|---|---|
| *B. cereus* 4415 | ATCC[a] |
| *B. cereus* JG-A30 | Haberlandhalde[b] |
| *B. sphaericus* 9602 | NCTC[c] |
| *B. sphaericus* JG-A12 | Haberlandhalde[b] |

a: American Type Culture Collection;
b: Isolate from the uranium mining waste pile Haberlandhalde, Johanngeorgenstadt, Germany;
c: National Collection of Type Cultures, London.

growth medium, the biomass was washed three times with 5 ml physiological NaCl-solution (0.9%).

For measurements of the phosphorus content of the bacterial cell walls, the following procedure was applied: Bacterial cells were mechanically disrupted by the use of a mixer-mill; the cell walls were separated from the cell debris by two consequent centrifugations at $400 \times$ g and $13\,000 \times$ g; approximately 20 mg/ml wet weight of bacterial cell walls were then chemically disintegrated with $HNO_3$ and $H_2O_2$ in a Floyd-MW microwave oven and finally resuspended in distilled water; and the phosphorus content in the resulting liquid phase was measured by ICP-MS spectrometry.

Two $4 \times 10^{-2}$ M U(VI) and U(IV) solutions in 1 M $HClO_4$ served as reference samples for the uranium oxidation states. The stock solution of U(VI) was obtained by dissolving $Na_2U_2O_7 \cdot 6H_2O$ in 7 M $HClO_4$. Part of this solution was reduced electrochemically to U(IV) at a mercury pool cathode. The uranium oxidation state in these solutions was confirmed by UV/Vis spectroscopy.

Bond length values were compared to those of uranium(VI) reference compounds to characterize the coordination of the uranium species formed on the *Bacillus* strains. Good agreement was found with structure parameters of inorganic uranyl phosphates (see below). Therefore, EXAFS measurements of different natural uranyl phosphates were carried out. These reference samples were copper uranyl phosphate (meta-torbernite) from Schneeberg/Germany, calcium uranyl phosphate (meta-autunite) from Autun/France and barium uranyl phosphate (meta-uranocircite) from Bergen/Germany. Their compositional and structural equivalence to the compounds reported in the literature was checked by energy-dispersive X-ray fluorescence spectroscopy (EDX) and X-ray powder diffraction (XRD) analysis. The chemical composition of the minerals agreed with the expected chemical formula. All three minerals occur in the meta-structure form.

## EXAFS measurements

Uranium $L_{III}$-edge XANES and $L_{II}$-edge EXAFS spectra of the *Bacillus*-uranyl species were measured in fluorescence mode on the wiggler beamline 4-1 at the Stanford Synchrotron Radiation Laboratory (SSRL) operating at 3 GeV and 40–90 mA. Uranium $L_{III}$-edge XANES spectra of the U(VI) and U(IV) reference solutions were obtained at the same beamline. The Si(220) double-crystal monochromator was used in channel-cut mode. Harmonic rejection was achieved by detuning of the second crystal relative to the first one, giving a $\sim 50\%$ intensity decrease of the incident flux. *Bacillus*-uranyl samples were loaded into polyethylene sample tubes and measured as wet pastes. The samples were measured 10–13 days after preparation. A four-pixel Ge fluorescence detector [5] was used for data collection. For each sample, three spectra were recorded and averaged. Deadtime correction was applied. The energy calibration at the uranium $L_{II}$ edge was carried out using the first inflection point in the derivative spectrum of a 0.054 M $UO_2(ClO_4)_2$ solution at 20 950 eV. We did choose the uranium $L_{II}$-edge because a monochromator glitch appeared in the energy region of the uranium $L_{III}$-edge EXAFS.

The EXAFS spectra of the uranyl phosphate reference samples were measured on the Rossendorf Beamline (ROBL) [6] at the European Synchrotron Radiation Facility (ESRF). The monochromator equipped with a Si(111) water cooled double-crystal system was used in fixed-exit mode. Higher harmonics were rejected by two Pt coated mirrors. A monochromator feedback control system [7] was used for stabilizing the intensity of the incident X-ray beam. The second mirror focused the beam vertically onto the sample. Uranium $L_{III}$-edge EXAFS spectra were collected in transmission using Ar-filled ionization chambers. For each sample, three spectra were measured and averaged. The samples were dispersed in 300 mg boron nitride and pressed as 1.3 cm diameter pellets. The amount of uranium used was calculated to give a jump of one across the uranium $L_{III}$-edge. Energy calibration of the uranium $L_{III}$-edge spectra was carried out using the first inflection point in the derivative spectrum of zirconium $K$-edge at 17 996 eV [8]. All measurements were taken at room temperature. Theoretical scattering phases and amplitudes were calculated with the scattering code FEFF6 [9] based on a 5 Å cluster using the crystal structure of $Cu[UO_2PO_4]_2 \cdot 8H_2O$ [10]. In addition to the U−O, U−C and U−P single-scattering paths, the four-legged multiple-scattering path $U-O_{ax1}-U-O_{ax2}-U$ of the uranyl moiety was calculated. The cluster calculation assumed a linear arrangement of the two axial oxygen atoms at a distance of 1.78 Å with respect to uranium. EXAFS fits were performed using a $k$-range of 2.8–13.8 $Å^{-1}$ for *Bacillus* strains and 2.8–14.0 $Å^{-1}$ for uranyl phosphate reference compounds. The value of the shift in threshold energy, $\Delta E$, was taken as a single variable for all coordination shells and was varied during the fits. The EXAFS spectra were analyzed according to standard procedures using the computer program EXAFSPAK [11]. The scaling factor, $S_0^2$, was set to 0.9.

## Results and discussion

The oxidation states of the uranium species after interaction with bacilli were analyzed using $L_{III}$-edge XANES features. Shape and edge-position of the X-ray absorption near-edge structure, XANES, is influenced by the oxidation state of the absorbing atom. Fig. 1 shows the uranium $L_{III}$-edge XANES spectra of solutions with $4 \times 10^{-2}$ M U(IV) and U(VI) in 1 M $HClO_4$. In comparison to the U(VI) solution, the white

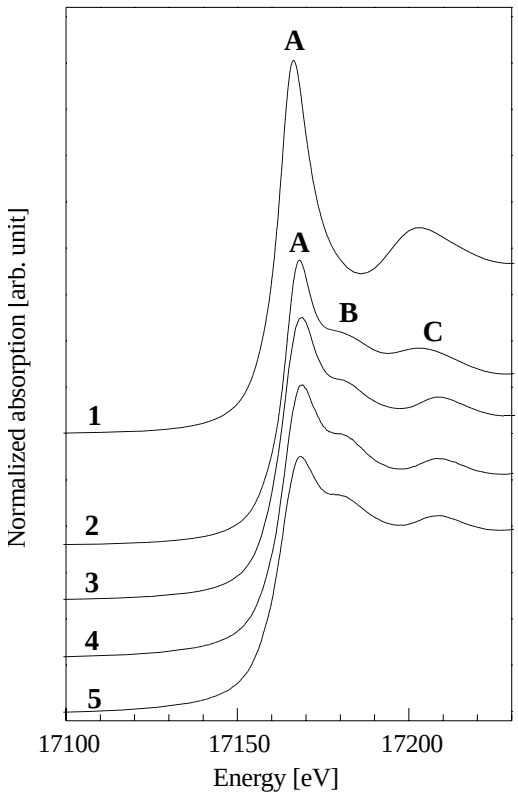


**Fig. 1.** Uranium $L_{III}$-edge XANES spectra of $4 \times 10^{-2}$ M U(IV) in 1 M $HClO_4$ (1), $4 \times 10^{-2}$ M U(VI) in 1 M $HClO_4$ (2), meta-autunite $Ca[UO_2PO_4]_2 \cdot 6H_2O$ (3), vegetative cells of *Bacillus sphaericus* JG-A12 with U(VI) (4) and spores of *Bacillus sphaericus* JG-A12 with U(VI) (5). The spectra were normalized to equal intensity at 17 230 eV.

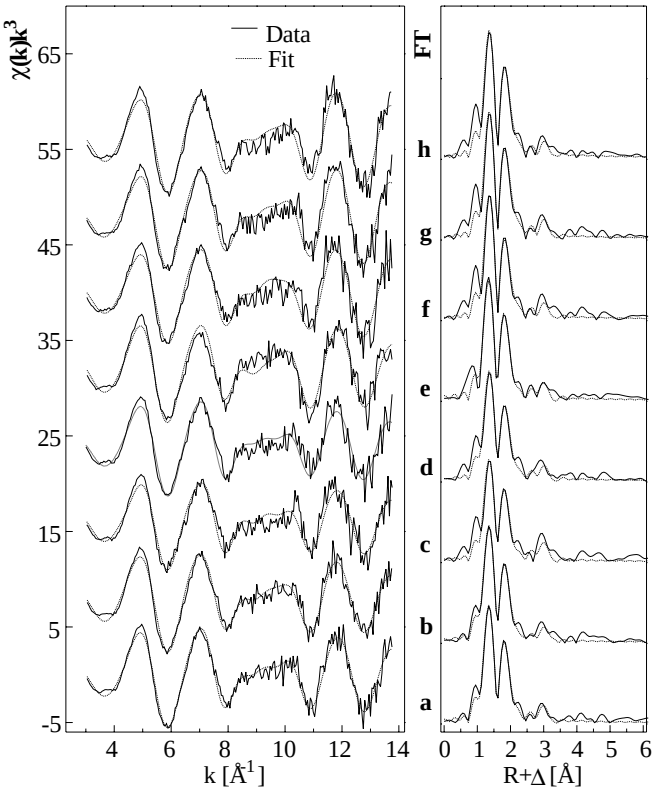


**Fig. 2.** Uranium $L_{II}$-edge $k^3$-weighted EXAFS spectra (left) and the corresponding Fourier transforms (right) of the *Bacillus*-uranyl complexes with vegetative cells from: *B. cereus* 4415 (a), *B. cereus* JG-A30 (b), *B. sphaericus* 9602 (c), *B. sphaericus* JG-A12 (d), and spores from: *B. cer*. 4415 (e), *B. cer*. JG-A30 (f), *B. sph*. 9602 (g) and *B. sph*. JG-A12 (h).

line intensity (A in Fig. 1) of the U(IV) XANES spectrum is increased and its energy is slightly reduced. Additional differences appear in the XANES features of the U(VI) samples above the white line (B in Fig. 1), which are interpreted in the literature by multiple-scattering effects of the axial atoms, $O_{ax}$, of the uranyl moiety [12, 13]. The observed spectral differences allow to distinguish between U(VI) and U(IV) oxidation states. As representative examples, the uranium $L_{III}$-edge XANES spectra of the uranyl species at vegetative cells and spores of *Bacillus sphaericus* JG-A12 are given in Fig. 1 as well. All bacilli samples show the typical pattern of U(VI) oxidation state. The XANES spectrum of the $Ca[UO_2PO_4]_2 \cdot 6H_2O$ reference compound shows also typical features of hexavalent uranium. In the spectra of the U(VI) samples, an additional peak (C in Fig. 1) is correlated with the bonding between uranium and its equatorial oxygen atoms, $O_{eq}$. The position of this peak is sensitive to this bond length. An increase in the distance between uranium and the $O_{eq}$ is associated with a shift of this peak to lower energy [14]. The short U−$O_{eq}$ bond distance in $Ca[UO_2PO_4]_2 \cdot 6H_2O$ and bacilli samples, shown later in this paper using EXAFS analysis, shifted peak C to higher energy as compared to the $4 \times 10^{-2}$ M U(VI) solution.

Uranium $L_{II}$-edge EXAFS spectra of the uranium species formed by the *Bacillus* strains and their corresponding Fourier transforms are shown in Fig. 2. The Fourier transforms (FT) represent radial distribution functions of the atoms surrounding the uranium atom. The FT's are not corrected for EXAFS phase-shifts, $\Delta$, causing peaks to appear at shorter distances ($R + \Delta$) relative to the real near-neighbor distances ($R$). The EXAFS equation was fit to the measured data using a structural model of two oxygen shells and one phosphorus shell. Without introducing any additional variable fit parameters, the multiple-scattering path of the uranyl moiety was linked to the U−$O_{ax}$ scattering parameters as described in [28]. The results of the data analysis are listed in Table 2.

In the vegetative cells and spores of the *Bacillus* samples, the uranium is coordinated by $O_{ax}$ at a distance of 1.78–1.79 Å. For the $O_{ax}$ atoms the coordination number is 1.8 to 2.3. The distance between uranium and $O_{eq}$ is 2.28–2.29 Å. The coordination number of the $O_{eq}$ atoms, $N_{eq}$, is determined to 4.4–5.7. The third peak, which is weaker in intensity, is a scattering contribution from phosphorus at a distance of 3.60–3.63 Å with a coordination number of 1.8–3.0. The small peak at $R + \Delta \approx 1$ Å in the FT is a typical relic of the subtracted spline-function. The EXAFS parameters of vegetative cells and spores are very similar, both for the uranium waste pile isolates and for the reference strains of *B. sphaericus* and *B. cereus*.

The U−$O_{eq}$ bond length depends strongly on the coordination geometry and is distinguishable for different coordination types. Steric effects and the number of ligands influence the bond lengths of each $O_{eq}$ atom. The average bond lengths, which are measurable with EXAFS, are indicative for the uranium coordination. The uranyl ion, $UO_2^{2+}$, can be coordinated by six, five or four oxygen atoms in the equatorial plane leading to hexagonal, pen-

**Table 2.** EXAFS structural parameters of *Bacillus*-uranyl complexes: vegetative cells of: *B. cereus* 4415 (**a**), *B. cereus* JG-A30 (**b**), *B. sphaericus* 9602 (**c**), *B. sphaericus* JG-A12 (**d**), and spores from: *B. cer.* 4415 (**e**), *B. cer.* JG-A30 (**f**), *B. sph.* 9602 (**g**) and *B. sph.* JG-A12 (**h**).

| Sample | Shell | $R$ [Å][a] | $N$[b] | $\sigma^2$ [Å$^2$][c] | $\Delta E$ [eV] |
|---|---|---|---|---|---|
| **a** | U−$O_{ax}$ | 1.78 | 2.1(2) | 0.0009 | −14.2 |
| | U−$O_{eq}$ | 2.28 | 5.4(4) | 0.0042 | |
| | U−P | 3.62 | 2.4(5) | 0.008[d] | |
| **b** | U−$O_{ax}$ | 1.79 | 2.3(2) | 0.0013 | −13.5 |
| | U−$O_{eq}$ | 2.28 | 5.2(4) | 0.0041 | |
| | U−P | 3.60 | 2.1(5) | 0.008[d] | |
| **c** | U−$O_{ax}$ | 1.79 | 1.8(2) | 0.0009 | −14.0 |
| | U−$O_{eq}$ | 2.28 | 5.1(6) | 0.0046 | |
| | U−P | 3.61 | 3.0(7) | 0.008[d] | |
| **d** | U−$O_{ax}$ | 1.79 | 2.1(2) | 0.0015 | −12.8 |
| | U−$O_{eq}$ | 2.28 | 4.9(5) | 0.0038 | |
| | U−P | 3.63 | 2.1(7) | 0.008[d] | |
| **e** | U−$O_{ax}$ | 1.78 | 1.9(2) | 0.0005 | −14.2 |
| | U−$O_{eq}$ | 2.28 | 5.7(5) | 0.0043 | |
| | U−P | 3.63 | 2.8(7) | 0.008[d] | |
| **f** | U−$O_{ax}$ | 1.79 | 2.1(2) | 0.0003 | −12.6 |
| | U−$O_{eq}$ | 2.28 | 4.6(6) | 0.0046 | |
| | U−P | 3.61 | 1.8(8) | 0.008[d] | |
| **g** | U−$O_{ax}$ | 1.79 | 2.1(1) | 0.0004 | −12.4 |
| | U−$O_{eq}$ | 2.29 | 4.4(4) | 0.0025 | |
| | U−P | 3.63 | 2.1(7) | 0.008[d] | |
| **h** | U−$O_{ax}$ | 1.79 | 2.0(2) | 0.0001 | −12.5 |
| | U−$O_{eq}$ | 2.29 | 4.7(5) | 0.0031 | |
| | U−P | 3.63 | 1.9(7) | 0.008[d] | |

a: Errors in distances are ±0.02 Å;
b: errors in coordination numbers are ±25% and standard deviations as estimated by EXAFSPAK are given in brackets;
c: Debye–Waller factor;
d: value fixed for the calculation.

tagonal or square bipyramidal coordination polyhedra. The structural classification for inorganic U(VI) compounds of Bruns (1996) *et al.* [15] showed that the average bond lengths are U−$O_{eq,\,hexagonal}$ = 2.46(12) Å, U−$O_{eq,\,pentagonal}$ = 2.34(10) Å, and U−$O_{eq,\,square}$ = 2.26(8) Å. The fivefold coordination with $O_{eq}$ is the most common geometry for organic U(VI) complex compounds [16, 17].

The U−$O_{eq}$ bond distances found in vegetative cells and spores of the *Bacillus* samples are 2.28–2.29 Å. In comparison to the structural parameters in the literature, this bond length is typical for an equatorial fourfold coordination. The small group of uranyl species that contain equatorial fourfold oxygen coordination will be discussed in the following part.

The hydrolysis reaction products of dioxouranium(VI) have been the subject of extensive studies. Most of the species have coordination numbers higher than four. One species, the $UO_2(OH)_4^{2-}$ ion, is fourfold coordinated by $O_{eq}$ atoms with a bond length of 2.26 Å [18, 19]. Because this hydrolysis species is insignificant at the pH range used and any excess uranium was removed by the washing procedure during the sample preparation, we can exclude the presence of hydrolysis species in the *Bacillus* samples.

Only a small number of organic uranyl complexes with an equatorial fourfold coordination exists. An equatorially fourfold coordinated organic compound is dibenzoatodioxouranium(VI), $UO_2(C_7H_5O_2)_2$ [20]. The structure is built up from infinite chains of uranyl centers bridged by carboxylic groups with an U−$O_{eq}$ distance of 2.282(8) Å. This bond length agrees with the U−$O_{eq}$ distance found for the bacilli samples. The weak peak, which appears in the FT's of the bacilli-uranyl complex samples at $R + \Delta = 3.0$ Å (Fig. 1) could be a result of U−C interaction. The U−C bond length in $UO_2(C_7H_5O_2)_2$, calculated from X-ray diffraction data given in [20], is 3.45 Å. A Fourier filter procedure including a subtraction of the other single-scattering contributions and the U−$O_{ax}$ multiple-scattering part was used to optimize the EXAFS fit of this weak feature at 3 Å. Using a cluster similar to $UO_2(C_7H_5O_2)_2$ for the calculation of scattering parameters, the hypothetical U−C distance in the spectra of the *Bacillus* samples was calculated to 3.47 Å. This is in agreement with the model. But there are two arguments against such an interpretation as U−C interaction. (a) The calculated carbon coordination number is even larger than five. This contradicts the fourfold coordination. (b) Most of the uranium(VI) compounds with carboxylic ligands coordinate in a monodentate or in a bidentate fashion. In both bonding types, the common coordination numbers $N_{eq}$ can be five or six, with exception of the above mentioned compound. A comparison with reference compounds showed, that the average U−$O_{eq}$ distance for monodentate ligation of the carboxyl group is nearly 2.39 Å, whereas the average distance for bidentate coordination is 2.48 Å [21]. These bond lengths are too large in comparison to the measured U−$O_{eq}$ values of the *Bacillus* strain samples. We, therefore, conclude that it is unlikely that the majority of the uranium is bound to carboxylate groups of the biomass.

Since we can exclude the carboxylate groups as origin of the weak peak at $R + \Delta = 3.0$ Å, it is necessary to consider the phosphoryl groups. In Gram-positive bacteria, and especially in bacilli, the most probable sites responsible for binding of many different metals are the phosphodiester residues of the so called secondary polymers consisting mainly of teichoic and teichuronic acids [22]. In addition, other bacterial cell surface polymers such as lipopolysacharides and phospholipides might also supply phosphoryl groups for metal binding [23]. The structure of the spore coat is completely different in comparison to the cell wall structure. The exosporium is dominated by negatively charged sites, which are most likely carboxylate but also phosphoryl groups [24]. The phosphoryl groups occur mainly in phospholipids, lipoteichoic and teichoic acids [25].

EXAFS data do not provide information on the absolute amount of uranium and phosphorus involved in the binding and contain only information about the main type of uranium coordination. Therefore, the phosphorus content was estimated in order to verify that there is enough phosphorus to bind the whole uranium. In our former work, it was demonstrated that the amount of uranium bound on the *Bacillus* cells in the EXAFS samples was in the range of 0.15 mmol U/g of dry weight of the biomass [4]. In addition, we found that the uranium is bound to the cell walls and not inside the cells. The walls of the *Bacillus* cells represent 15%–20% of the dry weight of the entire cells [26]. Therefore, the amount of uranium bound to the cell walls is 0.75 mmol U/g dry weight. In the present work, the phosphorus content of the cell walls of the *Bacillus* strains

studied was determined to be between 0.5 and 1.6 mmol P/g of dry weight. Despite the fact that not all phosphorus can be located at the cell surface, the analytical results show that a significant amount of phosphorus exists in the cell wall to bind the uranium.

Assuming a U−P shell in the EXAFS spectra of the *Bacillus* strain samples, the weak peak at $R + \Delta = 3.0$ Å can be reliably fit to a bond distance of 3.60–3.63 Å. The fit in this *R* region contains also a contribution of the $U-O_{ax}$ multiple-scattering path due to the very small Debye–Waller factor, $\sigma^2$, of the $U-O_{ax}$ coordination shell (Table 2). To have a better comparability of the U−P coordination numbers, $\sigma^2$ for this shell, which equaled 0.008 Å$^2$ for several samples, was held constant in all fits. The phosphorus coordination number for all bacilli samples ranges from 1.8 to 3.0.

A short $U-O_{eq}$ bond distance occurs when the $O_{eq}$ atoms of the uranyl polyhedron are at the same time the corners of four neighboring $XO_4$ tetrahedra. A stable coordination of this kind is formed by two-dimensional $[UO_2XO_4]$ sheets. The structural comparison of Bruns *et al*. [15] pointed out, that this $[UO_2XO_4]$ unit is built up only by $XO_4 = PO_4$ and $XO_4 = AsO_4$. A simplified picture of the uranyl phosphate structure is given in Fig. 3. Each uranium is connected with two double bonded oxygen atoms in the axial direction and surrounded equatorially by four oxygen atoms in a square planar arrangement. The $O_{eq}$ is at the same time the corner of a phosphate tetrahedra. Tetragonal dipyramidal coordinated uranyl ions and phosphate tetrahedra form two-dimensional layers. Both the short distance to $O_{eq}$ atoms and the phosphorus bond length and coordination number point to an uranyl structure in the *Bacillus* samples similar to the inorganic 1 : 1 uranyl phosphate species.

To corroborate the interpretation of the obtained structural parameters, EXAFS studies of inorganic phosphate compounds were performed. The natural minerals meta-torbernite $Cu[UO_2PO_4]_2 \cdot 8H_2O$ [10], meta-autunite $Ca[UO_2PO_4]_2 \cdot 6H_2O$ [27] and meta-uranocircite $Ba[UO_2PO_4]_2 \cdot 6H_2O$ [29] were used as samples. EXAFS spectra of the uranyl reference compounds measured at the uranium $L_{III}$-edge are depicted in Fig. 4. Fit results of data analysis are listed in Table 3. The

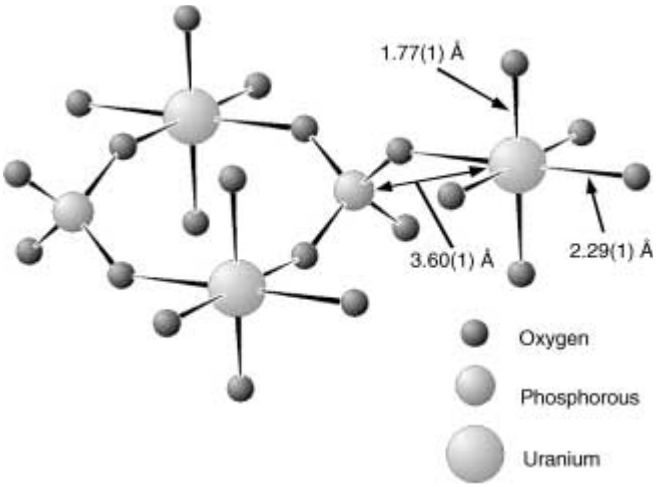


**Fig. 3.** Simplified structure of the 1 : 1 uranyl phosphate reference compounds showing a part of the uranyl phosphate layer. Typical distances from EXAFS measurements (see Table 3) with error limits are given for $U-O_{ax}$, $U-O_{eq}$ and U−P.

determined bond distances for the axial and equatorial U−O in the uranyl phosphates are 1.76–1.78 Å and 2.29 Å, respectively (Table 3). For comparison, the average bond lengths from X-ray diffraction measurements are also given in this table. In the higher *R*-range of the FT's, only scattering between the heavy atoms, phosphorus and uranium, are likely to be observed. The U−P distance in the uranyl phosphates obtained from the EXAFS spectra is 3.59–3.60 Å and the U−U distance is approximately 5.2 Å. Not detectable are the interlayer cations using EXAFS because their distances to the absorbing atom are too large. The Debye–Waller factors for the $O_{ax}$ atoms are higher than those for the $O_{eq}$ atoms because the axial atoms are not symmetry-equivalent. As a consequence, the $U-O_{ax}$ multiple-scattering path becomes very weak and does not contribute to the FT peak centered at 3 Å (Fig. 3). Therefore, the final fit was done without the multiple-scattering path.

The comparison with interatomic distances from single crystal structure data (Table 3) shows, that the EXAFS analysis gives the correct average bond length in each shell.

**Table 3.** EXAFS structural parameters for uranyl phosphate reference compounds: meta-torbernite $Cu[UO_2PO_4]_2 \cdot 8H_2O$ (**i**), meta-autunite $Ca[UO_2PO_4]_2 \cdot 6H_2O$ (**j**) and meta-uranocircite $Ba[UO_2PO_4]_2 \cdot 6H_2O$ (**k**). For comparison the averaged bond lengths based on single crystal structure data ($R_{XRD}$) from the literature are given.

| Sample | Shell | $R$ [Å][a] | $N$[b] | $\sigma^2$ [Å$^2$][c] | $\Delta E$ [eV] | $R_{XRD}$ [Å] | Ref. |
|---|---|---|---|---|---|---|---|
| **i** | $U-O_{ax}$ | 1.77 | 2.0(1) | 0.0042 | −11.1 | 1.81[e] | [10] |
| | $U-O_{eq}$ | 2.29 | 4.3(2) | 0.0028 | | 2.30 | |
| | U−P | 3.59 | 3.5(4) | 0.008[d] | | 3.59 | |
| | U−U | 5.2 | 3.4(7) | 0.008[d] | | 5.24 | |
| **j** | $U-O_{ax}$ | 1.76 | 2.2(1) | 0.0045 | −11.0 | 1.89[e] | [27] |
| | $U-O_{eq}$ | 2.29 | 3.9(2) | 0.0026 | | 2.32 | |
| | U−P | 3.60 | 2.3(3) | 0.008[d] | | 3.59 | |
| | U−U | 5.2 | 2.7(6) | 0.008[d] | | 5.23 | |
| **k** | $U-O_{ax}$ | 1.78 | 2.2(1) | 0.0049 | −9.3 | 1.78[e] | [29] |
| | $U-O_{eq}$ | 2.29 | 3.7(2) | 0.0021 | | 2.28 | |
| | U−P | 3.60 | 2.0(3) | 0.008[d] | | 3.58 | |
| | U−U | 5.2 | 2.8(6) | 0.008[d] | | 5.20 | |

a: Errors in distances are ±0.02 Å;
b: errors in coordination numbers are ±25% and standard deviations as estimated by EXAFSPAK are given in brackets;
c: Debye–Waller factor;
d: value fixed for the calculation;
e: Symmetry-inequivalent $U-O_{ax}$ bond lengths are averaged.

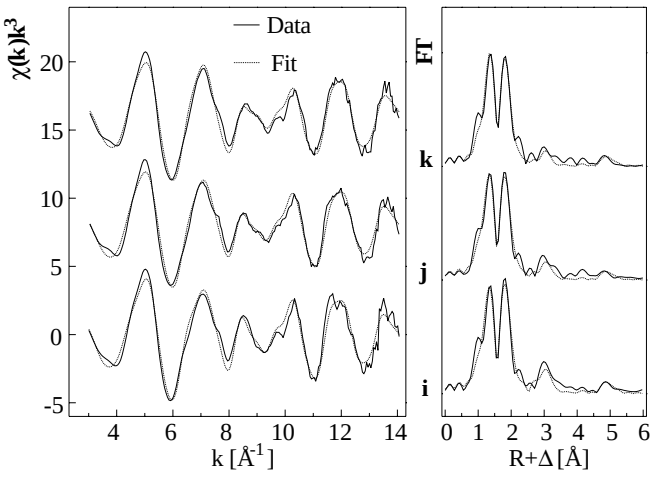


**Fig. 4.** Uranium $L_{III}$-edge $k^3$-weighted EXAFS spectra (left) and the corresponding Fourier transforms (right) of uranyl phosphate reference compounds: meta-torbernite $Cu[UO_2PO_4]_2 \cdot 8H_2O$ (i), meta-autunite $Ca[UO_2PO_4]_2 \cdot 6H_2O$ (j) and meta-uranocircite $Ba[UO_2PO_4]_2 \cdot 6H_2O$ (k).

The average U−$O_{ax}$ bond distance in meta-autunite obtained by XRD measurements is large in comparison to the EXAFS results. Single crystal X-ray diffraction measurements sometimes are complicated in the presence of heavy atoms, because these mainly determine the structure factors. This can lead to errors in the determination of atomic coordinates for light atoms [30]. The bond distances for meta-autunite given in Table 3 are in good agreement with the EXAFS measurements of Thompson *et al.* (U−$O_{ax}$ = 1.77 Å, U−$O_{eq}$ = 2.28 Å and U−P = 3.60 Å) [32].

The U−$O_{eq}$ bond length of the uranyl-*Bacillus* species agrees well with the bond length of these inorganic uranyl phosphate compounds. However, there are no metabolic processes kown that will liberate free phosphate groups available on surfaces of spores and vegetative cells of *B. sphaericus* and *B. cereus*. The U−P distance of 3.60–3.63 Å is typical for monodentate bound phosphate groups. In comparison to the inorganic uranyl phosphate compounds, the observed coordination number of $O_{eq}$ atoms is higher than four and the coordination number of phosphorus is lower than four. Furthermore, the EXAFS spectra of uranyl-*Bacillus* species and the 1:1 uranyl phosphate are different in the *k*-range 8–10 $Å^{-1}$ (see Figs. 2 and 4). It should be emphasized that this region is sensitive to polarization effects [31]. We did not detect any U−U interaction above the noise level. Therefore, the uranium could be surrounded in the bacilli samples by phosphoryl groups in a similar but not identical arrangement as in the inorganic 1 : 1 uranyl phosphate. However, some additional sites for uranium binding on non-phosphate groups at the bacterial cells wall cannot be excluded. In this case, the explanation of the experimental observations requires that some uranyl groups are sorbed on the bacterial surface with a different coordination geometry. However, these species contribute only weakly to the EXAFS signal. In the presence of significantly higher amounts of uranium(VI) with fivefold equatorial coordination bound to the bacteria cell wall, the U−$O_{eq}$ shell would be broadened due to additional contributions of longer U−$O_{eq}$ components. This would result in a larger $\sigma^2$ for the U−$O_{eq}$ shell. The fit to the EXAFS signal gives $\sigma^2$ between 0.0025 and 0.0046 $Å^2$ (Table 2) for the *Bacillus* strains. This is only slightly higher than the values for crystalline uranyl phosphate reference compounds (Table 3). The low $\sigma^2$ value for *Bacillus* strains indicates a high degree of structural order in the arrangement of the oxygen atoms in the equatorial plane. Therefore, we conclude that the amount of fourfold coordinated uranyl phosphates clearly exceeds the amount of other uranyl complex species with higher coordination numbers. EXAFS spectra of the uranium complexes in *Bacillus* vegetative cells and spores, which possess significant structural differences, are identical and indeed demonstrate the formation of structurally comparable uranyl phosphate species.

## Conclusions

The U $L_{III}$-XANES for all bacilli samples studied demonstrates that the uranium occurs in the U(VI) oxidation state. Because of the short U−$O_{eq}$ bond length and the presence of a weak U−P scattering contribution at a distance of 3.60 Å to 3.62 Å, we conclude that the EXAFS signal is determined mainly by monodentate bound phosphoryl ligands. For further investigations it is necessary to analyze organic reference compounds of uranyl complexes with phosphoryl residues using EXAFS and XRD. Identical structural parameters were obtained for uranium bound to both the vegetative cells and spores of *B. sphaericus* and *B. cereus* indicating that a structural similar uranium complex is formed on the cell walls.

*Acknowledgment.* This work was supported by grant No. 7531.50-03-FZR/607 from the Sächsisches Staatsministerium für Wissenschaft und Kunst, Dresden, Germany, and in part by the NATO Collaborative Research Grant No. SA.5-2-05(CRG.971641) 218/97/AHJ-501. We also acknowledge obtaining the mineral samples copper uranyl phosphate from the Staatliches Museum für Mineralogie und Geologie zu Dresden, collection number 7667Sy, calcium uranyl phosphate from J. Schöne, and barium uranyl phosphate from W. Enders. EXAFS measurements on *Bacilli* strains were made at SSRL, which is operated by the US Department of Energy, Office of Basic Energy Sciences, Division of Chemical Sciences and Materials Science. EXAFS measurements of reference compounds were made at the Rossendorf Beamline ROBL (BM20) at ESRF.

### References

1. Francis, A. J., Gillow, J. B., Dodge, C. J., Dunn, M., Mantioue, K., Streitelmeier, B. A., Pansoy-Hejelik, M. E., Papenguth, H. W.: Role of bacteria in the transport of actinides from deep underground radioactive waste repository. Radiochim. Acta **82**, 347 (1998).
2. Nakajima, A., Sakaguchi, T.: Selective accumulation of heavy metals by microorganisms. Appl. Microbiol. Biotechnol. **24**, 59 (1986).
3. Selenska-Pobell, S., Panak, P., Miteva, V., Boudakov, I., Bernhard, G., Nitsche, H.: Selective accumulation of heavy metals by three indigenous *Bacillus* strains, *B. cereus*, *B. megaterium* and *B. sphaericus*, from drain waters of a uranium waste pile. FEMS Microbiol. Ecol. **29**, 59 (1999).
4. Panak, P. J., Raff, J., Selenska-Pobell, S., Geipel, G., Bernhard, G., Nitsche, H.: Complex formation of U(VI) with *Bacillus*-isolates from a uranium mining waste pile. Radiochim. Acta **88**, 71 (2000).
5. Bucher, J. J., Allen, P. G., Edelstein, N. M., Shuh, D. K., Madden, N. W., Cork, C., Luke, P., Pehl, D., Malone, D.: A multichannel monolithic Ge detector system for fluorescence X-ray absorption spectroscopy. Rev. Sci. Instrum. **67**(9), 1 (1996).
6. Matz, W., Schell, N., Bernhard, G., Prokert, F., Reich, T., Claußner, J., Oehme, W., Schlenk, R., Dienel, S., Funke, H., Eichhorn, F.,

Betzl, M., Pröhl, D., Strauch, U., Hüttig, G., Krug, H., Neumann, W., Brendler, V., Reichel, P., Denecke, M. A., Nitsche, H.: ROBL – a CRG beamline for radiochemistry and materials research at the ESRF. J. Synchrotron Rad. **6**, 1076 (1999).
7. Krolzig, A., Materlik, G., Swars, M., Zegenhagen, J.: A feedback control system for synchrotron radiation double crystal instruments. Nucl. Instrum. Methods **219**, 430 (1984).
8. Kraft, S., Stümpel, J., Becker, P., Kuetgens, U.: High resolution X-ray absorption spectroscopy with absolute energy calibration for the determination of absorption energies. Rev. Sci. Instrum. **67**(3), 681 (1996).
9. Zabinsky, S. I., Rehr, J. J., Ankudinov, A., Albers, R. C., Eller, M. J.: Multiple-scattering calculations of X-ray-absorption spectra. Phys. Rev. B **52**, 2995 (1995).
10. Calos, N. J., Kennard, C. H. L.: Crystal structure of copper bis-(uranyl phosphate) octahydrate (metatorbernite), $Cu(UO_2PO_4)_2 \cdot 8H_2O$. Z. Krist. **211**, 701 (1996).
11. George, G. N., Pickering, I. J.: EXAFSPAK: A suite of computer programs for analysis of X-ray absorption spectra. Stanford Synchrotron Radiation Laboratory, Stanford, CA, USA (1995).
12. Petiau, J., Calas, G., Petitmaire, D., Bianconi, A., Benfatto, M., Marcelli, A.: Delocalized versus localized unoccupied $5f$ states and the uranium site structure in uranium oxides and glases probed by X-ray-absorption near-edge structure. Phys. Rev. B **34**, 7350 (1986).
13. Hudson, E. A., Rehr, J. J., Bucher, J. J.: Multiple-scattering calculations of the uranium $L_3$-edge X-ray-absorption near-edge structure. Phys. Rev. B **52**, 13 815 (1995).
14. Denecke, M. A., Reich, T., Bubner, M., Pompe, S., Heise, K. H., Nitsche, H., Allen, P. G., Bucher, J. J., Edelstein, N. M., Shuh, D. K.: Determination of structural parameters of uranyl ions complexed with organic acids using EXAFS. J. Alloys Comp. **271**–**273**, 123 (1998).
15. Bruns, P. C., Miller, M. L., Ewing, R. C.: $U^{6+}$ minerals and inorganic phases: a comparison and hierarchy of crystal structures. Can. Min. **34**, 845 (1996).
16. Evans, H. T.: Uranyl ion coordination. Science **141**, 154 (1963).
17. Leciejewicz, J., Alcock, N. W., Kemp, T. J.: Carboxylato complexes of the uranyl ion: effects of ligand size and coordination geometry upon molecular and crystal structure. In: *Structure and bonding*. (Clarke, M. J., *et al*. eds.) Springer, New York, Berlin, Heidelberg (1995).
18. Wahlgren, U., Moll, H., Grenthe, I., Schimmelpfennig, B., Maron, L., Vallet, V., Gropen, O.: Structure of uranium(VI) in strong alkaline solutions. A combined theoretical and experimental investigation. J. Phys. Chem. A **103**, 8257 (1999).
19. Clark, D. L., Conradson, S. D., Donohoe, R. J., Keogh, D. W., Morris, D. E., Palmer, P. D., Rogers, R. D., Tait, C. D.: Chemical speciation of the uranyl ion under highly alkaline conditions. Synthesis, structure and oxo ligand exchange dynamics. Inorg. Chem. **38**, 1456 (1999).
20. Cousson, A., Proust, J., Pagès, M.: Structure of Dibenzoatodioxouranium(VI). Acta Cryst. C **46**, 2316 (1990).
21. Denecke, M. A., Pompe, S., Reich, T., Moll, H., Bubner, M., Heise, K. H., Nikolai, R., Nitsche, H.: Measurements of the structural parameters for the interaction of uranium(VI) with natural and synthetic humic acids using EXAFS. Radiochim. Acta **79**, 151 (1997).
22. Doyle, R. J., Matthews, T. H., Streips, U. N.: Chemical basis for selectivity of metal ions by the bacillus subtilis cell wall. J. Bacteriology **143**, 471 (1980).
23. Brown, D. A., Beveridge, T. J., Keevil, C. W., Sherriff, B. L.: Evaluation of microscopic techniques to observe iron precipitation in a natural microbial biofilm. FEMS Microbiol. Ecol. **26**, 297 (1998).
24. Francis, C. A., Bradley, M. T.: Marine Bacillus spores as catalyst for oxidative precipitation and sorption of metals. J. Mol. Microbiol. Biotechnol. **1**, 71 (1999).
25. Murrell, W. G.: Chemical composition of spores and spore structures. In: *The bacterial spore*. (Gould, G. W., Hurst, A. eds.) Academic Press, London (1969).
26. Daniels, L., Hanson, R. S., Phillips, J. A.: Chemical Analysis. In: *Methods for General and Molecular Bacteriology*. (Gerhardt, P. ed.) American Society for Microbiology, Washington, D.C. USA (1994) pp. 512–554.
27. Makarov, E. S., Ivanov, V. I.: The crystal structure of meta-autunite, $Ca(UO_2)_2(PO_4)_2 \cdot 6H_2O$. Doklady Akademii Nauk SSSR **132**, 673 (1960).
28. Hudson, E. A., Allen, P. G., Terminello, L. J., Denecke, M. A., Reich, T.: Polarized X-ray-absorption spectroscopy of the uranyl ion: Comparison of experiment and theory. Phys. Rev. B **54**, 156 (1996).
29. Khosrawan-Sazedj, F.: The crystal structure of meta-uranocircite II, $Ba(UO_2)_2(PO_4)_2 \cdot 6H_2O$. Tscherm. Min. Petrogr. Mitt. **29**, 193 (1982).
30. Hennig, C., Reich, T., Funke, H., Rossberg, A., Rutsch, M., Bernhard, G.: EXAFS as a tool for bond-length determination in the environment of heavy atoms. J. Synchr. Rad. **8**, 695 (2001).
31. Hennig, C., Nolze, G.: Characterization of the preferred orientation in EXAFS-samples using Bragg-Brentano X-ray diffraction. In: *Speciation, techniques and facilities for radioactive materials at synchrotron light sources*. Workshop proceedings, Grenoble, 4–6 October 1998, NEA/OECD Paris (1999), pp. 235–243.
32. Thompson, H. A., Brown, G. E., Parks, G. A.: XAFS spectroscopic study of uranyl coordination in solids and aqueous solution. Am. Mineral. **82**, 483 (1997).